17th World Conference on Earthquake Engineering, 17WCEE
Sendai, Japan - September 27th to October 2nd, 2021

SEISMIC FRAGILITY SURFACE OF IRREGULAR REINFORCED CONCRETE FRAME STRUCTURES

A. Ghanem(1), D. Moon(2), Y.-J.. Lee(3)

(1) Ph.D. Student, University of Hawai'i at Mānoa, aghanem@hawaii.edu
(3) Assistant Professor, University of Hawai'i at Mānoa, dsmoon@hawaii.edu
(4) Associate Professor, Ulsan National Institute of Science and Technology (UNIST), ylee@unist.ac.kr

Abstract

Any change in the structure occupancy or use can significantly affect mass distributions in plan and elevation. The mass-eccentric structures having in-plan or vertical irregularities can suffer from non-uniform deformation demands due to the torsional effect. The existing design practices recommend special design requirements for such irregular structures to reduce additional seismic demands caused by torsion since they can result in significant live and economic losses during earthquake events. Many previous studies have conducted seismic vulnerability analyses of various irregular structures to understand their seismic behavior and quantity the failure likelihood under earthquake shaking. Because of the prevailing challenge of extreme computational expense in the frailty analysis, many researchers have utilized simplified 2D analytical models for their studied structures. However, overly idealized models often cannot reflect the true structural behavior under seismic loads, especially when any structural irregularity exits in the system. Yet, the use of more detailed models in earthquake simulations may not be practically possible with existing methods. Also, almost all previous studies have adopted three or four failure limit states in the vulnerability analysis and have derived corresponding seismic fragility curves; however limited numbers of fragility curves could not deliver the complete seismic vulnerability information of the structures. This research investigates seismic performance of reinforced concrete frame structures that have vertical or in-plan irregularities from the change in the structure use. Fourteen prototype models are developed by assuming different live load distributions in elevation or plan. Unlike other studies, 3D detailed analytical models are employed for numerical simulations and a total of eight limit states are utilized based on the allowable drift ratio. A new fragility curve derivation method is introduced which couples the structural analysis and reliability analysis to derive efficient yet accurate vulnerability curves with the first-order reliability method. A series of nonlinear dynamic response history analysis is conducted with ten earthquake ground motions; all seismic fragility curves are successfully obtained using personal computers. The functional representations of the derived curves are reported for designers and engineers. The term "seismic fragility surface" is firstly introduced in this study. The fragility surface is constructed from the fragility curves at all limit states, and it offers the thoroughgoing vulnerability relationship of the structure to the earthquake loading. The direct effects of vertical and in-plan irregularities on the structural performance of the studied reinforced concrete frames are clearly shown from the obtained fragility curves and surfaces.

Keywords: seismic vulnerability; irregularity; fragility curve; fragility surface; eccentric mass, FORM

1. Introduction

Earthquakes are one of the deadliest natural disasters. More than eight hundred thousand fatalities are caused by earthquakes that occurred from 2000 to 2015 globally [1]. Moreover, they often cause severe economic loss. A study reports that earthquakes in the United States result in about 4.4-billion-dollar loss annually [2]. From post-earthquake damage investigations, researchers find out that buildings with structural irregularity suffer the most. However, irregular building structures represent a significant percentage of the modern urban infrastructure. Irregularity in the structures is rooted in uneven distributions of their mass, stiffness, or strength. Any change in the use or occupancy of building structures can significantly affect the mass distribution in plan and vertically (in elevation); the eccentric mass distribution generally increases the structural irregularity in the system. As lateral load resisting members in eccentric structures experience non-uniform deformation demands due to the torsional effect, irregular structures should be analyzed and designed with proper detailed analytical models which can represent their complicated structural behaviors. The structural irregularity can be categorized into two groups, which are vertical irregularity and plan irregularity. The in-plan irregularity occurs when the center of the mass is away from the center of rigidity. The seismic inertia loads act through the center of the mass, and the restoring forces by lateral load-resisting members act at the center of rigidity. The differences in the mass and rigidity centers introduce torsional moments, causing the structure to rotate about the center of rigidity. The vertical irregularities are induced by different story heights, building geometry setback, column offsets, and non-uniform mass on each floor. Even when in-plan or vertical irregularities are not presented at the initial design, regular building structures can become mass-eccentric structures depending on how to use that structure.

In previous studies on the seismic vulnerability assessment of irregular structures, many researchers have developed seismic fragility curves using the Monte Carlo simulation (MSC). As the structural failure is a relatively low probability event, the MCS method frequently requires thousands or millions of simulations to obtain one failure event, and it substantially suffers from high computational time and cost. So, researchers often simplify their studied structures to save the computational expense, and idealized 2D analytical models are regularly utilized in the analysis. However, the use of overly simplified models may not truly reflect the actual structural behavior under seismic loading. On the other hand, some researchers have derived the fragility curves by calculating structural failure probabilities mathematically from analytically derived limit state functions. This approach is referred as the analytical function-based method, and it usually does not require any earthquake simulations. Still, the complexity of the structure is idealized, reducing the accuracy of the calculated failure probabilities.

This study investigates the seismic response of reinforced concrete moment frame structures having varied vertical and in-plan irregularities due to the change in the building's use. 3D structural models are developed with different mass distributions in plan and vertically. To overcome the computational challenge in the seismic vulnerability analysis with 3D analytical models, a new method is adopted which can draw the fragility surface with high accuracy yet low computational cost. Nonlinear dynamic response history analyses are conducted to derive the complete vulnerability relationship for all studied models. Cumulative log-normal functions are assumed to fit the obtained fragility curves, and their parameters are reported. The term "fragility surface" is introduced, and it is constructed with all derived fragility curves; so, it shows the failure probabilities in terms of earthquake intensities and allowable drift ratios.

2. Seismic Fragility Analysis Method

Since earthquakes cause catastrophic structural damages and economical losses, many research efforts have been devoted to assessing the seismic vulnerability of various structures and mitigate the expected seismic risk. For this, seismic fragility curves are widely used as they are essential in seismic risk assessment and loss estimation. Seismic fragility curves describe the probability of failure of a structure based on predefined damage conditions under the earthquake hazard. They show the probability of failure versus the ground intensity measure such as peak ground acceleration and give the inventory percentage that will suffer from that event.

There are two dominant approaches to develop seismic fragility curves. The first approach is based on analytical functions of limit states, and failure probabilities are calculated as the probability of reaching the predefined limit state condition in which the structural capacity is less than the seismic response or demand. In this method, the limit state function is required to be analytically expressed using random variables. The use of this method is extremely limited as deriving the closed-form limit state function is practically impossible for detailed models and with advanced structural analysis methods. Thus, the second approach is more popular, which is the simulation-based method. This method calculates failure probability by dividing the number of failure cases by the total number of simulation cases. The failure is defined where the simulated structure response reaches or exceeds the predefined damage state criteria [4]. In this method, any advanced structural analysis techniques (e.g., inelastic pushover or dynamic response history analysis) can be used. One of the major shortcomings of this approach (e.g., MCS) is that conducting a large number of simulations can be extremely computationally expensive.

There have been many studies in assessing the effect of the vertical irregularity on the seismic performance of building structures using fragility curves. Hanan Al-Nimry studied building structures with vertical stiffness irregularities by using simple 3D analytical models [5]. The analytical function-based method was utilized in the vulnerability analysis. N. Achaean et al. analyzed vertically irregular buildings with a soft story in various heights [6]. 2D simplified models were adopted, and fragility curves were derived analytically from the limit state functions. Nari et al. compared regular and irregular moment-resisting concrete and steel 2D frames with various irregularities [7]. The research used the analytical function-based method to determine the failure likelihood. Bhosale et al. examined various irregular building structures [8]. All structures were modeled as 2D frames, and their seismic fragility curves are analytically derived. Mohammad et al. evaluated strength irregular buildings using 2D analytical models [9]. The failure probabilities were calculated from the MCS.

In this study, a state-of-the-art structural reliability analysis method is introduced and utilized to generate seismic fragility curves economically and more precisely. This new method integrates both structural and reliability analysis tools to reduce the computational cost and increase the accuracy of the result [10]. The structural analysis software ZEUS-NL and reliability analysis tool FERUM (Finite Element Reliability Using MATLAB) are combined with the linking tool FERUM-ZEUS [11] developed in MATLAB. Under this framework, ZEUS-NL performs structural analysis, and FERUM calculates the failure probability based on the first-order reliability method (FORM). MATLAB serves as a platform expediting the calculation process with parallel computing techniques that allow multiple analyses to be performed simultaneously. The overall fragility analysis process is presented in Fig. 1.

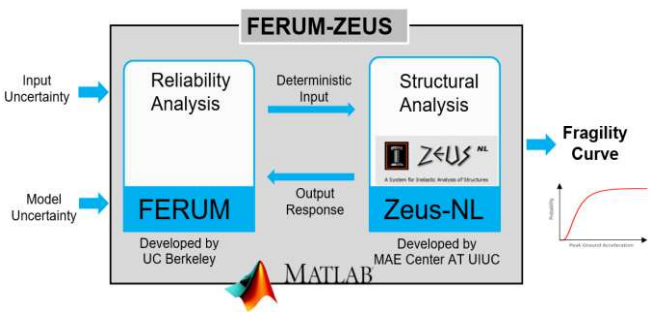

Fig. 1 – Integrated Fragility Analysis Framework

3. Analytical Models and Input Earthquakes

The target structures are 3-story ordinary reinforced concrete moment frames with three bays and three frames. The selected structures are designed mainly for gravity loads and are not prepared for earthquake events; but they represent a large portion of office buildings in the United States. 3D analytical models of the

target structures are created in the ZEUS-NL. Fig. 2 shows the FEM model with all structural nodes. There are 48 reinforced concrete columns with a square cross-section of 12-inch width. Beams are modeled with reinforced concrete T section with a depth of 18 inches and a slab thickness of 6 inches.

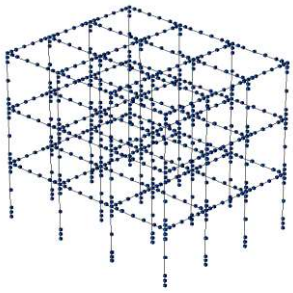

Fig. 2 – Structural Model in ZEUS-NL

There are some uncertainties in actual material strengths. Many factors can change the compressive strength of concrete, such as the temperature change, curing method, and vibration method. Thus, in this study, steel and concrete strengths are modeled as random variables. According to Dr. Bartlett and Dr. MacGregor, the true compressive strength of concrete material can be assumed to follow the log-normal distribution [12]. Another similar research reports that steel reinforcement also follows the same distribution [13]. The log-normal distribution parameters for concrete and steel materials used in the analysis are summarized in Table 1.

Table 1 –Log-normal Distribution Parameters for Material Properties

Material	Mean	Standard Deviation
Concrete	33.6 MPa	0.186
Steel	336.5 MPa	0.107

It is assumed that the total mass in the structure remains constant while the live load distribution can be changed. As the studied structures are office buildings, the live load of 50 pounds per square foot (psf) is accepted according to the ASCE 7-16 design code [14]. In this study, fourteen different live load distribution scenarios are considered, and they are grouped into two categories. The first category includes seven models, which are vertically irregular mass-eccentric models with uniformly distributed live loads on each floor plan (referred as VIMEU) having seven distinct vertical distribution cases. The second category includes the other seven models, which are vertically irregular mass-eccentric models with concentrated live loads on the half of each floor plan (referred as VIMEH). The vertical load distribution cases are the same as the first category, but this group has the in-plan irregularity as well as the vertical irregularity. The difference in the in-plan live load distribution (shown in yellow color) and the corresponding in-plan eccentricities are presented in Fig. 3. The seven vertical live load distribution scenarios are shown in Fig. 4. All loads are applied as concentrated forces determined from the two-way slab tributary method.

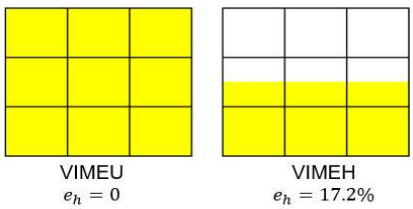

Fig. 3 – In-plan Live Load Distribution

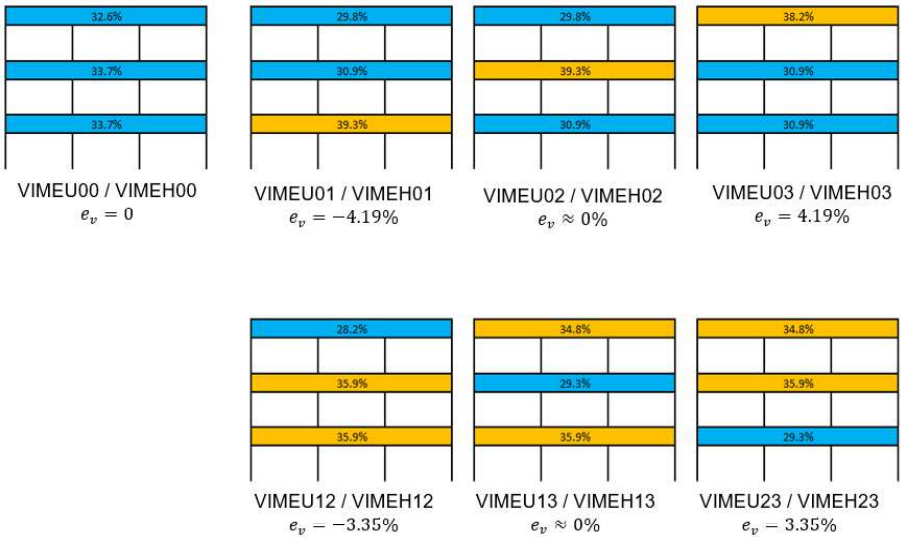

Fig. 4 – Vertical Live Load Distribution

Ten earthquake records that can characterize diverse types of earthquakes are used for the seismic analysis. The ground motions are carefully selected based on the ratio of peak ground acceleration to the peak ground velocity to simulate possible earthquake loads acting on the structure. The chosen ground motion acceleration records are displayed in Fig. 5, and Fig. 6 exhibits their elastic response spectra and the average response spectrum (shown in the thick red line).

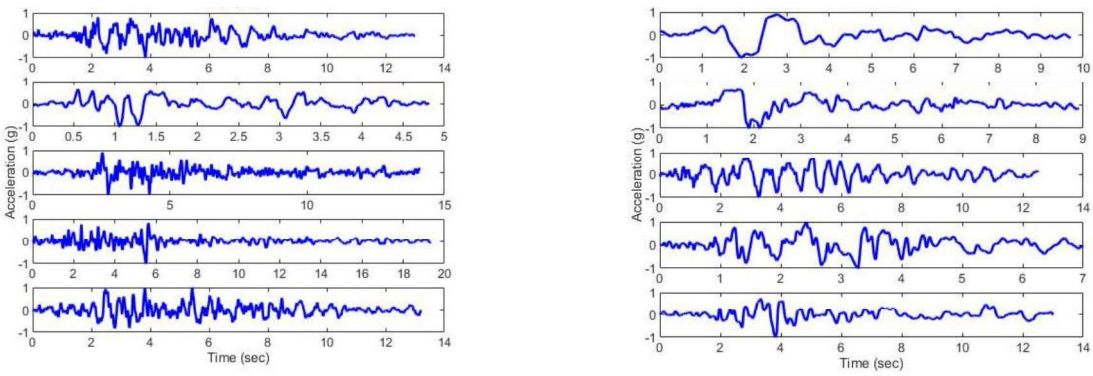

Fig. 5 – Earthquake Records

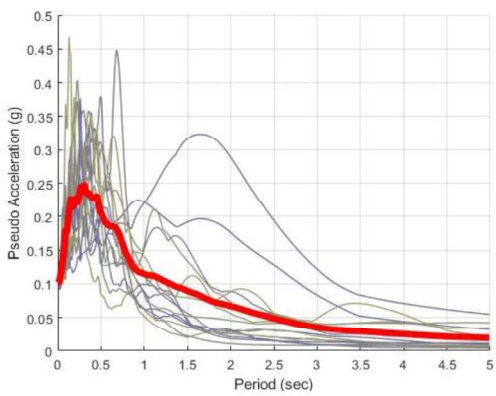

Fig. 6 – Elastic Response Spectra

4. Seismic Fragility Analysis

In the proposed fragility analysis, a dynamic response history analysis is conducted in ZEUS-NL, and the structural analysis results are sent to FERUM for the reliability analysis. In order to determine whether the structure fails according to the predefined damage condition, the limit state criteria that quantify the seismic capacity are typically obtained from the pushover analysis. Instead, this study adopts eight limit states based on the maximum allowable drift ratio values, which are 0.25%, 0.50%, 0.75%. 1.00%, 1.25%, 1.50%, 1.75% and 2.00%. The fragility curves at eight limit states are combined to draw the fragility surface. The use of eight limit states rather than typically employed three or four limit states is practically possible as the proposed method is highly computationally efficient.

In this study, fourteen prototype 3D frame models are analyzed with ten earthquake records and eight limit state definitions. This sums up to a total of 1120 cases. To decrease computation time, a modification is made so that parallel computing can be incorporated into the analysis. The total computation time is reduced to two weeks to derive all fragility curves with two ordinary personal computers with six Intel i7 CPU cores. The fragility analysis does not generate the fragility curve automatically; it provides a series of data points following a specific trend. A regression analysis is followed to determine analytical fragility curve functions assuming the log-normal cumulative distribution.

4.1. Fundamental Periods

The eigenvalue analysis is performed for all studied models, and Fig. 7 compares their first natural periods. The result shows that the models of VIMEU03/VIMEH03 and VIMEU23/VIMEH23 have longer periods than the other models, which coincides with the expectation that more loads on higher floors result in a more flexible system. Also, it is expected that those models would suffer more from the increasing overturning moment.

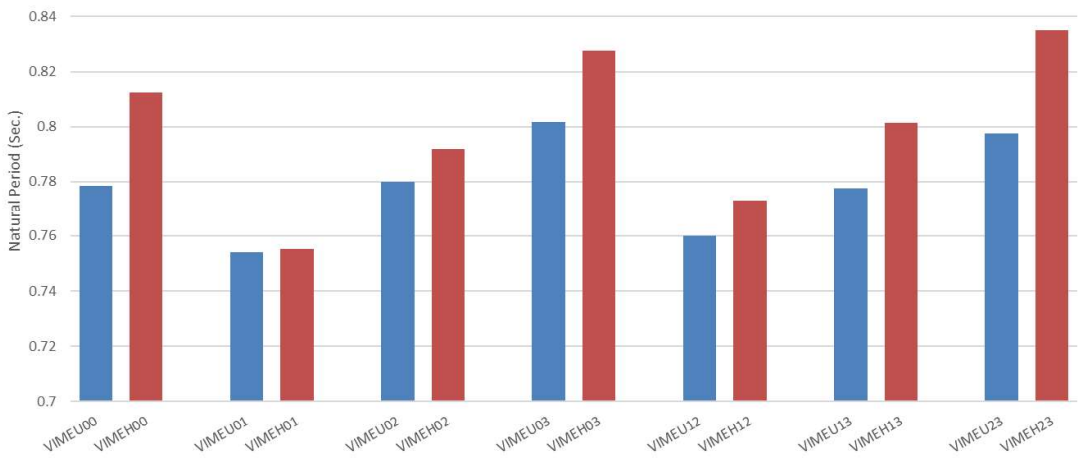

Fig. 7 – Fundamental Periods of Studied Models

4.2 Fragility Curves

Under the proposed framework, seismic fragility curves for studied reinforced concrete frame structures with vertical and in-plan irregularities are successfully derived. Fragility curves are assumed to be cumulative log-normal distribution functions, and they are obtained from the least square curve fitting. Selected fragility curves are shown in Fig. 8, and each plot has smoothed fragility curves for eight limit states. The figure legend is based on the model reference name and the allowable drift ratio of the limit state. The fragility curve of the 0.25% limit-state is moved to the left of one of the 2.00% limit-state. It is noteworthy that seismic fragility curves are greatly affected by the structural irregularity in elevation as well as in plan. A list of log-normal parameters of derived fragility curves for all studied models is reported in Table 2.

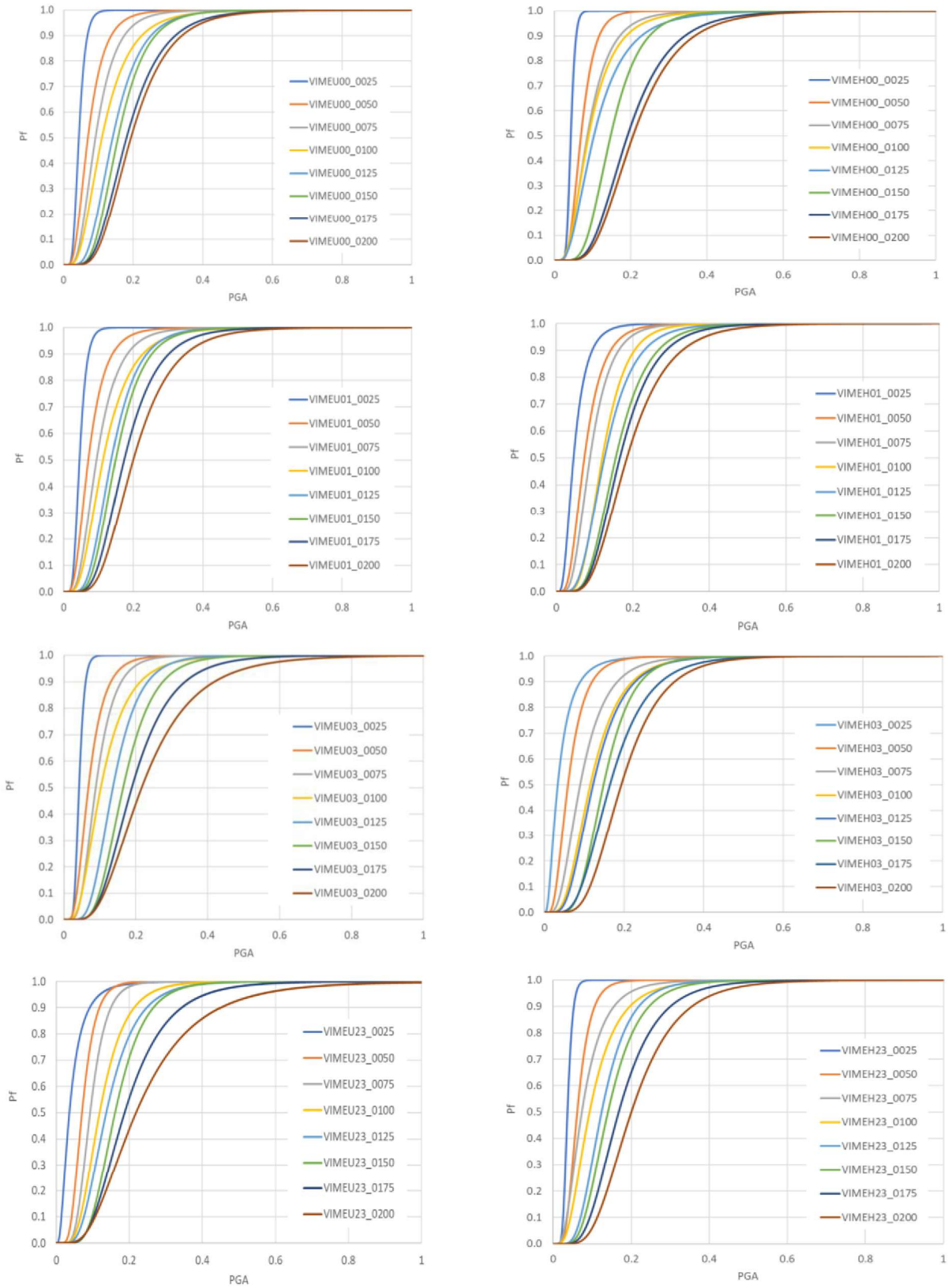

Fig. 7 – Selected Fragility Curves

Table 2 –Fragility Curve Log-normal Parameters

Model	Parameters	Limit State							
		0.25%	**0.50%**	**0.75%**	**1.00%**	**1.25%**	**1.50%**	**1.75%**	**2.00%**
VIMEU00	Mean	0.0459	0.0796	0.1033	0.1281	0.1555	0.1695	0.1996	0.2283
	Variance	0.0003	0.0020	0.0031	0.0060	0.0055	0.0052	0.0089	0.0118
VIMEU01	Mean	0.0488	0.0820	0.1081	0.1315	0.1547	0.1626	0.1908	0.2201
	Variance	0.0003	0.0022	0.0035	0.0059	0.0048	0.0049	0.0075	0.0102
VIMEU02	Mean	0.0612	0.0740	0.0891	0.1145	0.1345	0.1587	0.1786	0.2004
	Variance	0.0011	0.0019	0.0041	0.0060	0.0049	0.0042	0.0084	0.0140
VIMEU03	Mean	0.0434	0.0770	0.0980	0.1203	0.1458	0.1782	0.2089	0.2466
	Variance	0.0002	0.0018	0.0023	0.0056	0.0068	0.0055	0.0099	0.0185
VIMEU12	Mean	0.0667	0.0857	0.1120	0.1379	0.1559	0.1661	0.1993	0.2245
	Variance	0.0017	0.0021	0.0050	0.0054	0.0050	0.0059	0.0092	0.0104
VIMEU13	Mean	0.0523	0.0838	0.1005	0.1323	0.1505	0.1801	0.2057	0.2337
	Variance	0.0007	0.0019	0.0032	0.0045	0.0046	0.0088	0.0099	0.0123
VIMEU23	Mean	0.04683	0.0765	0.0994	0.1319	0.1525	0.1740	0.2096	0.2561
	Variance	0.0016	0.0010	0.0015	0.0040	0.0055	0.0050	0.0111	0.0244
VIMEH00	Mean	0.0438	0.0754	0.0995	0.1057	0.1251	0.1602	0.2123	0.2283
	Variance	0.0001	0.0010	0.0033	0.0045	0.0072	0.0047	0.0102	0.0118
VIMEH01	Mean	0.0533	0.0840	0.0989	0.1311	0.1407	0.1698	0.1821	0.2045
	Variance	0.0011	0.0021	0.0025	0.0032	0.0048	0.0056	0.0066	0.0094
VIMEH02	Mean	0.0612	0.0740	0.0891	0.1145	0.1345	0.1587	0.1786	0.2004
	Variance	0.0012	0.0012	0.0023	0.0053	0.0062	0.0052	0.0068	0.0084
VIMEH03	Mean	0.0452	0.0689	0.1050	0.1312	0.1377	0.1598	0.1822	0.2103
	Variance	0.0016	0.0017	0.0040	0.0051	0.0051	0.0040	0.0074	0.0081
VIMEH12	Mean	0.0612	0.0820	0.0929	0.1153	0.1358	0.1525	0.1618	0.2021
	Variance	0.0023	0.0028	0.0028	0.0060	0.0066	0.0057	0.0055	0.0124
VIMEH13	Mean	0.0274	0.0688	0.0912	0.1139	0.1350	0.1637	0.1903	0.2040
	Variance	0.0013	0.0010	0.0018	0.0054	0.0050	0.0050	0.0081	0.0092
VIMEH23	Mean	0.0385	0.0677	0.0874	0.1105	0.1371	0.1545	0.1863	0.2215
	Variance	0.0001	0.0009	0.0031	0.0049	0.0041	0.0050	0.0079	0.0108

The limit state function is defined as the structural supply (or capacity) minus seismic demand (or response). When the limit state function is much larger than zero, the structure would not fail as there is enough seismic capacity for the expected seismic demand (i.e., the supply is much larger than the demand). In fact, the limit state function value is closely related to the failure probability. Fig. 8 plots the failure likelihood versus the initial limit state function for the selected model. As expected, the failure probability increases with the decrease of the limit state function, and this shows the relation between differences in

seismic supply and demand and failure probabilities. Note that the computational cost can be saved considerably by limiting the fragility analysis within the range of the trend line and by assuming the failure probability outside this range as either 0 or 1.

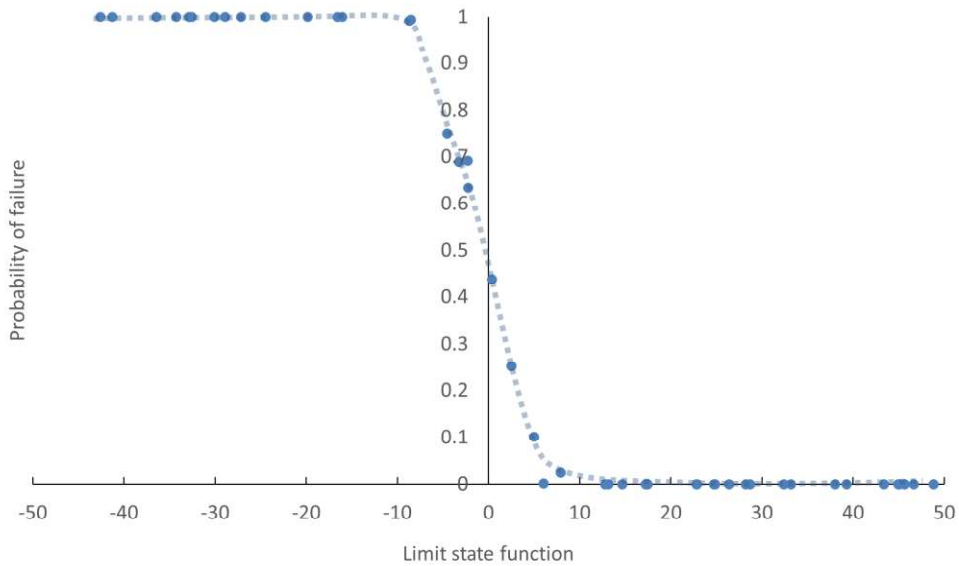

Fig. 8 – Failure Probability vs. Limit State function (VIMEU03 Model with 1.75% Limit State)

To assess the impact of mass irregularity on seismic performance, a VIMEH model having high vertical irregularity is compared to the VIMEH model that does not have any vertical irregularity. Fig. 9 shows fragility curves for VIMEH00 and VIMEH03 models at the limit state of the 1.00% allowable drift ratio. The VIMEH03 model has much higher failure probabilities when compared with the VIMEH00 model. It appears that at the peak ground acceleration of 0.16g, the probability of failure of VIMEH03 is 10% higher than that of VIMEH00.

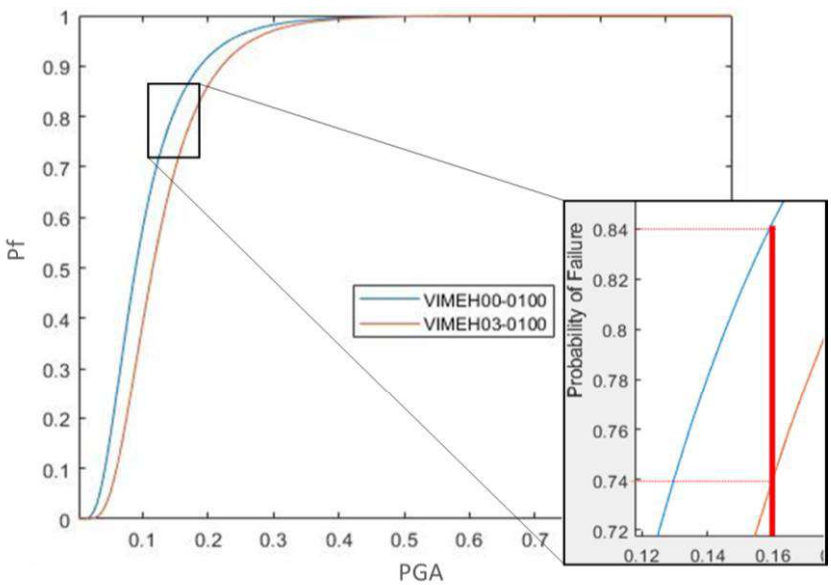

Fig. 9 – Effect of Vertical Irregularity on Fragility Curves

Fig. 10 compares fragility curves of VIMEU13 and VIMEH13 models with eight different limit states. This clearly shows that the in-plan irregularity makes the reinforced concrete frame structures more susceptible to earthquake loading, as repeatedly found in the previous studies.

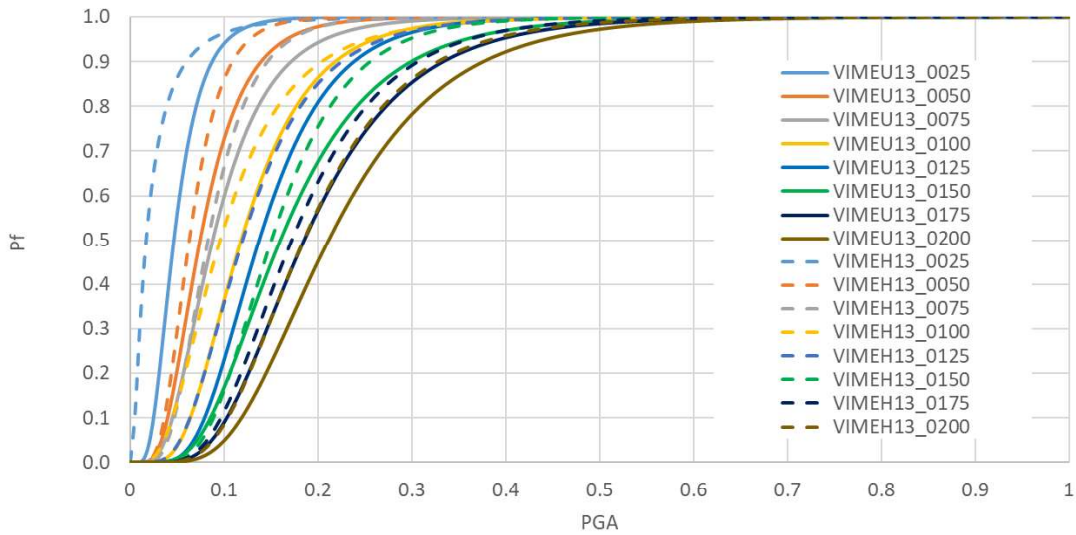

Fig. 10 – Effect of In-plan Irregularity on Fragility Curves

4.3. Fragility Surfaces

Fig. 11 plots the seismic fragility surfaces of selected reinforced concrete frame structures with vertical and in-plane irregularities. The fragility surface is constructed from the derived fragility curves for all eight limit states. As visibly shown, the different levels of in-plan and vertical irregularities produce meaningly different seismic fragility surfaces. The failure probability increases with the stricter damage state definition. If any simulation-based method such as MCS is applied to the same vulnerability analysis, it would be practically impossible to derive the facility surface owing to the extremely expensive computational cost.

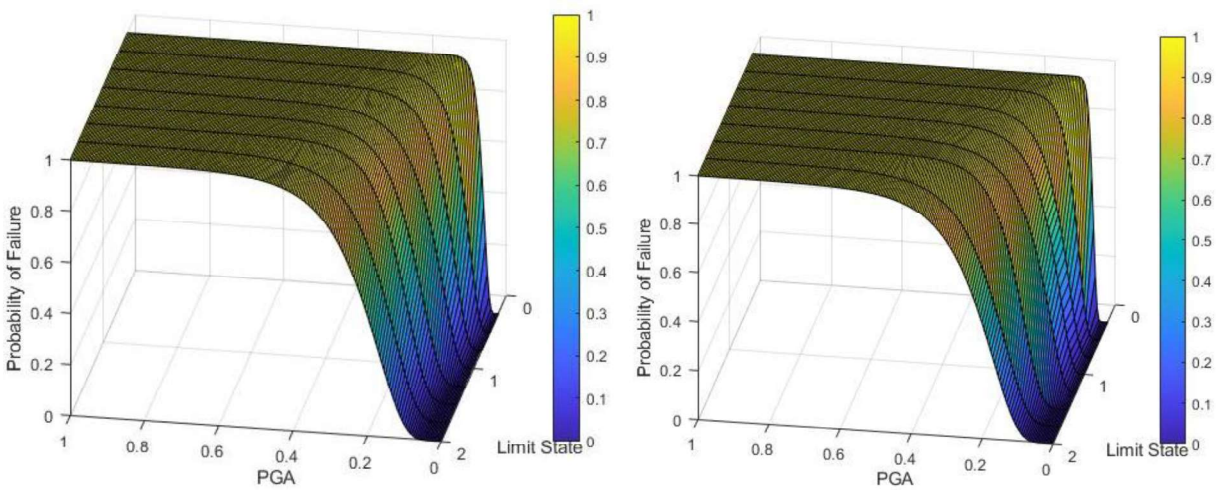

(a) VIMEU00 Model (b) VIMEH00 Model

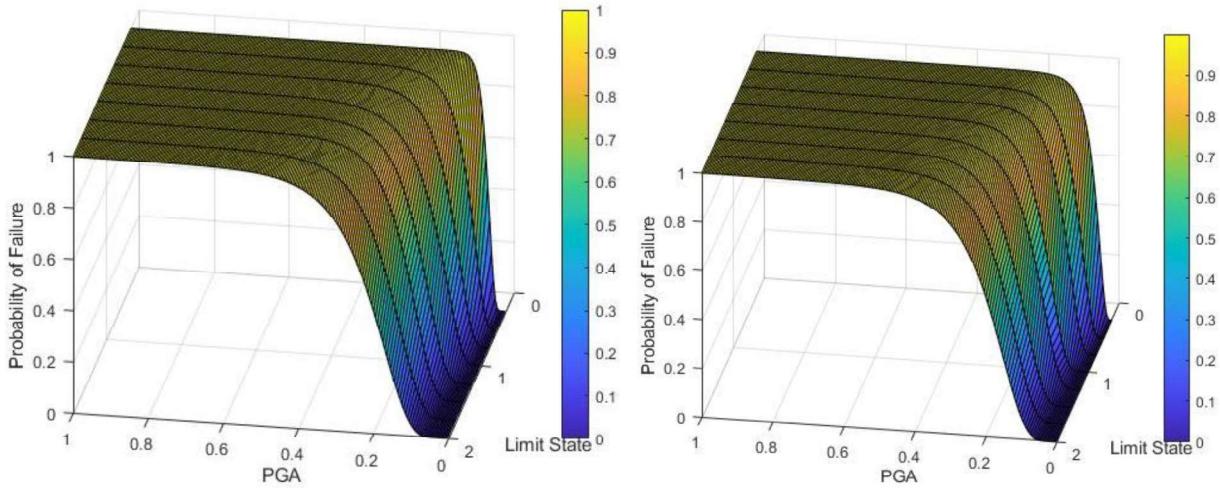

(c) VIMEU01 Model

(d) VIMEH01Model

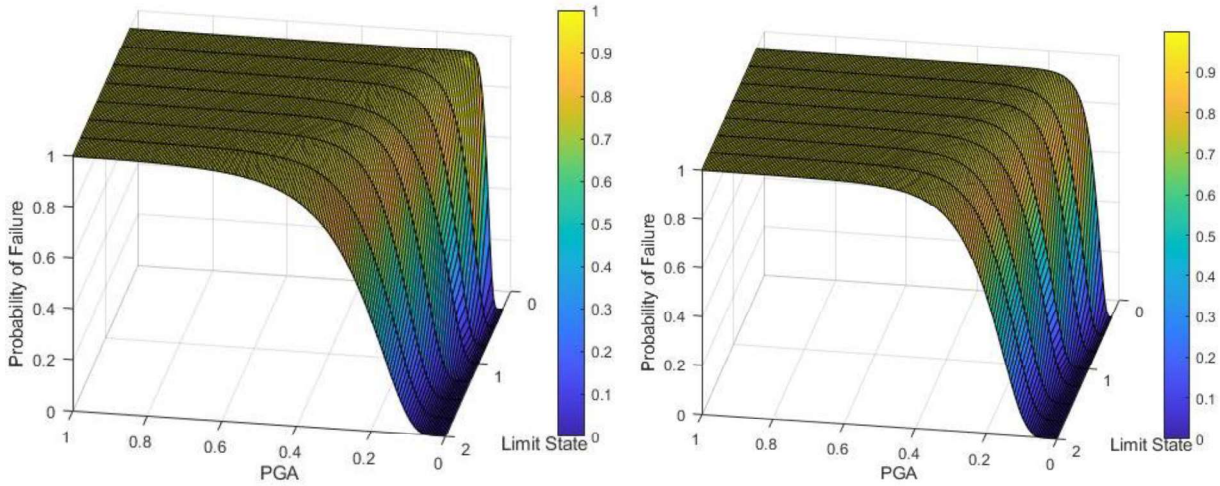

(e) VIMEU03 Model

(f) VIMEH03 Model

Fig. 10 – Selected Fragility Surface

5. Summary

Three-story ordinary concrete reinforced moment-resisting frames are analyzed. An attempt is made to obtain seismic fragility curves in a precise and efficient way. An integrated structural reliability analysis method is adopted to perform seismic vulnerability analysis to overcome the computational challenge in the use of 3D analytical models. The concrete and steel strengths are modeled as random variables that follow the log-normal distribution. Fourteen different live-load distribution scenarios are considered. Ten earthquake ground motion records are selected for nonlinear response history analysis. Eight limit states based on the allowable drift ratio are assumed. A total of 1120 cases are explored on two ordinary personal computers. 112 fragility curves are generated, and seismic fragility surfaces are drawn from them. The proposed method is proven to efficiently produce seismic fragility curves even with the computationally demanding 3D analytical models. The use or occupancy change can convert initially regular structures to mass-eccentric systems having irregularities in plan or elevation, making more vulnerable to earthquake loads; the direct effects of vertical and in-plan irregularities on the seismic performance are confirmed from the derived fragility curves and surfaces. The log-normal cumulative functional forms of the vulnerability

curves are provided for the design of irregular reinforced concreted frame structures. The seismic surface, firstly introduced in this study, provides the comprehensive information about structural performance under the earthquake events.

6. References

[1] Annual US earthquake losses estimated at $4.4B. (n.d.). Retrieved November 30, 2020, from https://www.govcon.com/doc/annual-us-earthquake-losses-estimated-at-44b-0001.

[2] Department, P., & 30, S. (2016, September 30). Deaths due to earthquakes worldwide 2000-2015. Retrieved November 30, 2020, from https://www.statista.com/statistics/263108/global-death-toll-due-to-earthquakes-since-2000/.

[3] Kwon, O. S., & Elnashai, A. S. (2007): Fragility analysis of a bridge with consideration of soil-structure-interaction using multi-platform analysis. In Structural Engineering Research Frontiers (pp. 1-14).

[4] Melchers RE (1999): Structural reliability: analysis and prediction. 2nd Edition, John Wiley, New York, NY.

[5] Hanan Al-Nimry. 2019. "Development of Seismic Fragility Curves of RC Infilled Frame Buildings in Jordan." Matec Web of Conferences 281 https://doi.org/10.1051/matecconf /201928101012.

[6] Hamzeh Shakib, Mehdi Nodeh, and Farashad Homaei. 2015. "Fragility Curve Development for Assessing Midrise Steel buildings with Buckling Resistant Braced System Having Vertical Irregularity. JSEE Vol 17, No.4.

[7] Fang, N., & Westcott, B. (2018, May 12). A decade on, heartache of deadly Sichuan quake still being felt. Retrieved December 09, 2020, from https://www.cnn.com/2018/05/11/asia/sichuan-earthquake-anniversary-intl/index.html.

[8] Avadhoot Bhsale, Robin Davis, and Pradip Sarkar. 2018. "New Seismic Vulnerability Index for Vertically Irregular Buildings." ASCE-ASME. J. Risk Uncertainty Eng. Syst., Part A: Civ. Eng., 4(3): 04018022.

[9] VU. Unnikrishnan, A.M. Prasad and B.N. RAO. 2013. "Development of fragility curves using high-dimensional model representation." Earthquake Engng Struct. Dyn. 2013; 42:419-430.

[10] Lee, Young Joo, and Moon, Do Soo. 2014. "A new methodology of the development of seismic fragility curves." Smart Struct. Syst. 14 (5): 847–867. https://doi.org/10.12989/sss.2014.14.5.847.

[11] Moon, Do Soo & Lee, Young Joo & Lee, Sangmok. 2018. Fragility Analysis of Space Reinforced Concrete Frame Structures with Structural Irregularity in Plan. Journal of Structural Engineering (United States). 144. 10.1061/(ASCE)ST.1943-541X.0002092.

[12] Bartlett, F. M., and J. G. Macgregor. 1996. "Statistical analysis of the compressive strength of concrete in structures." ACI Mater. J. 93 (2): 158–168.

[13] Mirza, S. A., and J. G. MacGregor. 1979. "Variability of mechanical properties of reinforcing bars." J. Struct. Div. 105 (5): 921–937.

[14] American Society of Civil Engineers. 2017. Minimum design loads and associated criteria for buildings and other structures: ASCE/SEI 7-16.

